A Stepwise Data Interpretation Process For Renal Amyloidosis Subtyping by LMD-MS

Ming Ke
Guangzhou KingMed Center for Clinical Laboratory Co.,Ltd.
Xin Li
Guangzhou KingMed Center for Clinical Laboratory Co.,Ltd.
Lin Wang
Guangzhou KingMed Center for Clinical Laboratory Co.,Ltd.
Shuling Yue
Guangzhou KingMed Center for Clinical Laboratory Co.,Ltd.
Beibei Zhao (lab-zhaobeibei@kingmed.com.cn)
Guangzhou KingMed Center for Clinical Laboratory Co.,Ltd.

Research Article

Keywords: Amyloidosis, Laser microdissection, Mass spectrometry, Proteomics

Posted Date: October 13th, 2021

DOI: https://doi.org/10.21203/rs.3.rs-917392/v1

Abstract

Backgrounds: Systemic amyloidosis is classified according to the deposited amyloid protein, which determines its best therapeutic scheme. The laser microdissection combined with mass spectrometry (LMD-MS) technique is a promising approach for precise subtyping of amyloidosis, however, is hampered by how to interpret the MS data.

Objectives: The objective of the present study is to establish a complete data interpretation procedure for LMD-MS based amyloidosis subtyping.

Methods: Formalin fixed paraffin-embedded specimens from patients with renal amyloidosis were analyzed by LMD-MS for proteome quantification. Forty-two specimens were used for training the data interpretation procedure, which was validated by another 50 validation specimens. Area under receiver operating curve (AUROC) analysis of amyloid accompanying proteins (APOE, APOA4 and SAMP) for discriminating amyloidosis from non-amyloid nephropathies was performed.

Results: A stepwise data interpretation procedure that include or exclude the subtypes group by group was established, in which, involvement of non-immunoglobulin amyloid protein is determined by P-score, involvement of immunoglobulin light chain is determined by variable of λ-κ, and immunoglobulin heavy chain's participation is judged by H-score. This data interpretation method achieved a 88% accuracy in 50 validation specimens. The amyloid accompanying proteins showed significant quantitative differences between amyloidosis specimens and non-amyloid nephropathies. Each of the single accompanying protein had a AUROC value more than 0.9 for diagnosis of amyloidosis from non-amyloid control, and the averaged value of spectral count of the three accompanying proteins showed the highest AUROC (0.966), indicating it might be an alternative indicator for amyloidosis diagnosis.

Conclusions: The proteomic data interpretation procedure for amyloidosis subtyping based on LMD-MS was established successfully, which has high clinical application value.

Background

Systemic amyloidosis is a group of heterogeneous diseases caused by protein structural abnormality. The pathological character of amyloidosis is the formation of extracellular deposition of beta-sheet fibril through aggregation of insoluble proteins or peptides. The cytotoxicity of the deposited proteins cause destruction of tissue and cellular structure, which then induce functional injury of organs, the kidney, for example, is the most commonly affected organ, and eventually lead to diseases [1–3]. Systemic amyloidosis is classified according to the type of deposited protein, these mainly include immunoglobulin light/heavy chain, and other non-immunoglobulin amyloidogenic proteins [3–8]. The major affected organs, prognosis and effective treatment strategies of each amyloidosis subtype are different [9–12], therefore, precise subtyping is of paramount importance for providing patients with the most appropriate care.

For diagnosis of amyloidosis, histopathologic examination methods are mostly used in routine practice, such as histochemical stain by Congo red (CR) [13]. Further subtyping methods are usually based on immunohistochemistry and immunofluorescence, which rely heavily on antibody recognition that might be problematic as the result of background interference and epitope loss [14]. In 2008, Mayo Clinic proposed the laser microdissection combined with mass spectrometry (LMD-MS) technique for amyloidosis subtyping [15], and it gradually becomes the gold standard in recent years[3]. MS-based assay has a lot of advantages, for example it can detect multiple targets in one tissue section at one time, whereas for antibody-based immunoassay, it has to utilize an array of antibodies to recognize different targets with multiple tissue sections consumed in multiple tests [16, 17].

However, there is still a gap between the LMD-MS technology itself and its transition to clinical application, that is largely due to the uncertainty of how to interpret the MS data. As proposed by Mayo Clinic, the subtype of amyloidosis is called by considering the most abundant amyloid protein that has the maximal MS/MS spectral count (SC) (Mayo's rule) [18–20]. Nevertheless, in routine practical detection, due to the complexity of MS data that multiple amyloid proteins are often identified at the same time, when the deposition degree of the pathogenic amyloid protein is not that significantly superior to others, or blood contamination happens, or due to little amount of material from microdissection, the pathogenic protein may not have an absolute preponderance of SC when compared with other amyloid proteins in the background, which makes it challenging to make a precise subtyping diagnosis by simply extracting the protein with the highest SC. For instance, IgG is often identified with high SC in immunoglobulin light chain amyloidosis (AL) [21]. In Leukocyte chemotactic factor-2 amyloidosis (ALECT2), previous empirical data showed that the SC of LECT2 is generally low, not to mention to get the highest SC [22]. What's more, comparison of protein SC within a specimen is not a quantitative method that has comparability between different samples. Thus, it may need a global normalization method for establishing a relatively unified quantitative analysis system.

The prevalence rate of different amyloidosis subtypes vary greatly in different regions, but anyway, AL is always the most popular one (59%-68%); serum amyloid A amyloidosis (AA, 4-12%), ALECT2 (~3%) and transthyretin amyloidosis (ATTR, 3%-33%) could be considered as sub-popular subtypes; whereas the other subtypes are rare [1, 23, 24]. In AL, κ-type (ALκ) and λ-type (ALλ) interfere with each other, mainly because of the high background of κ chain; In terms of subtyping fibrinogen α chain amyloidosis (AFib), the SC of FIBA should be greater than the sum of fibrinogen β chain (FIBB) and fibrinogen γ chain (FIBG) in addition to the requirement of the highest SC of FIBA among all amyloid proteins [25]; and as mentiioned above, ALECT2 is a special existence. Besides, special considerations are required for making definite diagnosis of immunoglobulin heavy chain amyloidosis (AH) and its involvement with AL, that is immunoglobulin heavy-light chain amyloidosis (AHL) [26]. Thus, it is reasonable to propose a stepwise process to include or exclude the subtypes of specific amyloidosis patient. In this study, we aimed to establish an LMD-MS based amyloidosis subtyping procedure, especially for the rules of MS data interpretation.

Another important aspect of utilization of LMD-MS in amyloidosis is the detection and quantification of accompanying proteins that are co-deposited with amyloid fibrils. So far as we know, three proteins named apolipoprotein E (APOE), apolipoprotein A-IV (APOA4), and serum amyloid P component (SAMP) are usually accompanied with amyloid deposition in amyloidosis. Although the LMD-MS analysis is usually executed based on histopathologic diagnosis, that is usually a positive staining of CR, the three accompanying proteins are often regarded as the evidence of amyloid deposition. Even, the criterion of detection of at least two of the three accompanying proteins has been considered to be surrogate for CR staining [27]. However, whether the diagnostic criterion is feasible in more clinical specimens needs to be tested, and alternative ways that may improve the diagnostic performance needs further investigation.

Methods

Clinical specimens

A total of 92 formalin fixed paraffin-embedded (FFPE) renal puncture specimens of systemic amyloidosis that were diagnosed in *Department of Pathology, Guangzhou KingMed Diagnostics* were collected, of which 42 retrospective specimens received from January 2018 to December 2019 were used for method training, and 50 from January 2020 to June 2021 were collected for method validation. These specimens were required to meet the following criteria: clinical manifestations of renal or other organ dysfunction; CR staining was positive and apple-green birefringence was observed under polarized light; unbranched and randomly arranged fibrous at 8-12nm under electron microscopy; CR positive fibrillary glomerulonephritis was excluded by the marker DNAJB9 [28]. The amyloidosis subtypes of the cases were characterized by immunofluorescence, immunohistochemistry, Immuno-electron microscopy, serum and urine test of immunofixation electrophoresis and serum free light chain, the results were reviewed by three senior licensed pathologists. We also collected other 55 specimens that were non-amyloid nephropathies as control. This study has been approved by the Ethics Committee of *Guangzhou KingMed Diagnostics* and meets the ethical requirements.

Specimen preparation and laser microdissection

FFPE tissue specimen was cut into 7 μm sections, which were then removed onto a specialized POL-membrane for microdissection on a steel frame slide. Sections were then air dried, melted, and deparaffinized. After that, CR staining was conducted to identify positive areas of amyloid deposition. The selected CR positive micro area were dissected using the Leica LMD6 system. A 0.5 mL centrifuge tube prefilled with 40 μL lysate buffer (10 mM Tris, 1 mM EDTA, 0.5% NaDOC) on the cap was used to collect the micro pieces. A total of at least 200 000 μm^2 dissection area of each specimen was required.

Peptide sample preparation

The collected micro piece was centrifuged to the bottom of the tube, followed by ultrasonication for 15 min, incubation at 98 ℃ for 1 h to de-crosslink proteins, and ultrasonication again for 15 min. Protein was then digested by 0.5 ug trypsin (Promega) at 37℃ for 4h or overnight. The generated peptide was

reduced by 5 mM dithioethylitol at 37°C for 30 min, and alkylated by 15 mM iodoacetamide at room temperature in dark for 45 min. Trifluoroacetic acid was added to terminate the reaction, followed by centrifugation at 20 000 *g*, the supernatant was collected. The Ziptip C18 column (Millipore) was used for desalination of the peptide solution. The eluted peptide mixture was then dried by a vacuum-frozen concentrator and redissolved with 0.1% trifluoroacetic acid in water before MS analysis.

LC-MS/MS analysis and data retrieval

The peptide mixture was subjected to the Ultimate 3000 RSLC nanoLC, separated by online reversed-phase chromatography, and then injected into the Q Exactive mass spectrometer (Thermo Scientific) via Nano-ESI source. MS data was firstly converted to mgf file by ProteoWizard and then retrieved by Mascot software (Matrix Science), suing the protein database of *Home sapiens* from Swissport. The retrieval parameters were set as follows: Enzyme: Trypsin/P; Allow up to: 2 missed cleavages; Fixed modifications: Carbamidomethyl (C); Variable modifications: Oxidation (M); peptide tol.: 10 PPM, MS/MS tol.: 0.02 Da. The PSM (peptide-spectrum-match) hit was re-scored by Percolator, and the retrieval results were filtered using the Proteome Discoverer software (Thermo) under the following conditions: FDR < 1%, Number of peptides matched ≥ 2.

Protein quantification and statistical analysis

The relative abundance of a target protein was evaluated by its normalized SC, which was calculated through the following formula: $NC_i = C_i / \sum_{k=1}^{n} C_k \times 1000$. Where NC_i is the normalized SC of protein i, C_i is the absolute SC in MS raw data, and n is the number of all identified proteins. The abundance of amyloid proteins were calculated accordingly. To calculate the superiority of the pathogenic amyloid protein over others, the superiority score (S-score) of each of the amyloid proteins was defined as: S- $score_i = NC_i/Max(NC_{-i})$. Where $Max(NC_{-i})$ was the maximum normalized SC of the reset amyloid proteins other than protein i. The λ-κ value for judging immunoglobulin light chain involvement was calculated by: $\lambda\text{-}\kappa = NC_{Ig\lambda} - NC_{Ig\kappa}$. And the superiority of immunoglobulin heavy chain over light chain (H-score) was defined as: $\text{H- score} = NC_j / Max(NC_{Ig\kappa}, NC_{Ig\lambda})$. Where protein j was limited to IgG, IgA or IgM. Wilcoxon rank test was used to analyze the significance of difference between paired SC of Igk and Igλ within a group, and Mann-Whitney U test was used to analyze the significance of difference between groups.

Results

Demographics of the study cohort

To establish the amyloidosis subtyping procedure, FFPE tissue specimens from 42 renal amyloidosis patients were collected, including 9 ALκ, 12 ALλ, and 21 relatively sub-popular and rare subtypes (4 cases of ALECT2, 3 of each of AHL (IgGλ) and AHL (IgAλ), 2cases of each of AH (IgG), AA and gelsolin

amyloidosis (AGel), and 1 case of each of AHL (IgGκ), AFib, ATTR, apolipoprotein A1 amyloidosis (AApoAI) and lysozyme amyloidosis (ALys)). A total of other 50 cases were included in validation set for testing the performance of the amyloidosis subtyping procedure. Among them, 13 and 17 subjects were diagnosed as ALκ and ALλ, as well as 5 cases of AHL (IgGλ), 3 cases of each of AH (IgG), AGel, ALECT2 and AHL (IgAλ), 2 cases of AA and 1 case of ATTR (Table 1). Additionally, the study included a set of control specimens that are non-amyloid nephropathy (diabetic nephropathy (DN, n = 13), focal glomerulonephritis (FGN, n = 8), IgA nephropathy (IgAN, n = 9), lupus nephritis (LN, n = 5), membranous nephropathy (MN, n = 15) and para-carcinoma (pC, n = 5). The clinical information for the subjects is listed in Table 2.

Table 1
Clinically confirmed subtypes of traning and validation dataset

Amyloidosis subtype	Training set	Validation set
ALκ	9	13
ALλ	12	17
AHL (IgGκ)	1	0
AHL (IgGλ)	3	5
AHL (IgAλ)	3	3
AH (IgG)	2	3
AA	2	2
AGel	2	3
ALECT2	4	3
ATTR	1	1
AFib	1	0
AApoAI	1	0
ALys	1	0
Total	42	50

Table 2
Clinic Characteristics of the Subjects

	Training set	Validation set	Non-amyloid nephropathy					
			DN	FGN	IgAN	LN	MN	pC
Age (years)	60.0 (52.0-64.0)	61.0 (51.8-67.3)	56.0 (51.0-60.0)	43.0 (39.0-46.8)	41.0 (31.0-42.0)	34.0 (29.0-38.0)	51.0 (45.0-56.0)	-
Gender (male/female)	22/20	31/19	6/7	2/6	3/6	0/5	12/3	5*
Upro (mg/day)	3482 (1731-7490)	3716 (2755-5687)	3835 (2658-8013)	3480 (2740-5340)	1060 (815-1690)	3583 (2142-6214)	3984 (3720-4248)	-
Alb (g/L)	22.9 (17.8-28.3)	25.7 (20.7-29.3)	27.4 (25.1-32.2)	31.8 (28.9-33.4)	38.8 (38.7-39.0)	26.2 (24.0-29.7)	16.8 (15.8-17.7)	-
Scr (μmol/L)	84.0 (58.0-141.0)	85.0 (68.5-100.0)	108.0 (60.0-191.0)	64.0 (57.0-99.0)	82.0 (67.0-92.0)	64.0 (59.0-68.0)	93 (85.5-100.5)	-
BUN (mmol/L)	6.0 (5.4-9.0)	7.3 (4.5-9.2)	5.4 (4.4-7.7)	4.7 (3.3-6.2)	5.6 (5.2-7.0)	5.4 (3.6-5.5)	5.0 (3.4-5.8)	-
*Clinical information of pC specimen was not collected.								
Data are presented as median with interquartile range.								
Abbreviations: Upro, urine protein; Alb, albumin; Scr, serum creatinine; BUN, blood urea nitrogen.								

Characteristics of spectral count distribution of amyloid proteins in training dataset

ALECT2

ALECT2 has been reported as a special existence that it could be principally determined as long as LEC2T is identified at the deposition site [14]. Our result also showed that LECT2 only presented in ALECT2 cases with relatively lower abundance as compared to other amyloid proteins, and was almost absent from the deposit of non-ALECT2 amyloidosis (Fig. 1a). The S-score of LECT2 in ALECT2 was just a little bit beyond 0, but none of them was above 1 (Fig. 1b). Therefore, the identification or failure to identify LECT2 could be used as a criterion to include or exclude ALECT2, but don't have to require it having the highest SC.

AFib/AApoAI/AGel

The SCs of FIBA, apolipoprotein A-I (APOA1) and GELS also showed irregular patterns that they were observed to be relatively high in the background across the training specimens (Fig. 1a and

Supplementary Fig. 1a, c, e), which may interfere the identification of other subtypes if Mayo's rule utilized (Supplementary Fig. 1b, d, f). Consistent with previous report [25], the SC of FIBA was found to be significantly greater than the sum of FIBB and FIBG in AFib, while only a few cases have slightly higher SC of FIBA than the sum of FIBB and FIBG in non-AFib (Fig. 1c). The S-score of FIBA in AFib was 7.92, but in non-AFib, it had a median of 0.42 (IQR, 0.22 - 0.52), and the cut-off could be set to 4.60, which was the mean of the highest score in none-AFib (1.28) and the score in AFib (7.92) (Fig. 1d). Similarly, the SC of APOA1 was surprisingly high in AApoAI (Supplementary Fig. 1c), thus the criterion for this subtype should be stricter. The median S-Score of APOA1 was 0.34 (IQR, 0.25 - 0.52) in non-AApoAI, whereas in AAPOAI it was 10.96, the cut off could be 6.12 accordingly (Fig. 1e). Whereas for AGel, the S-score of GELS of the two cases in training set were 2.41 and 1.77, which were significantly higher than in non-AGel, 0.32 (IQR, 0.17 - 0.43), and the cut off could be 1.41 (Fig. 1f).

AA/ATTR/ALys

Serum amyloid A-1 (SAA1) was seldomly observed in non-AA cases, while transthyretin (TTHY) and lysozyme C (LYSC) were identified frequently across the training specimens (Fig. 1a). Anyhow, these three amyloid proteins each showed evident SC superiority than others in their related amyloidosis subtype, and the opposite inferior position in their unrelated subtypes. These results indicated that these three subtypes could be determined via the Mayo's rule (Supplementary Fig. 2a-c).

ACys/Aβ2M/AApoAII/AApoCII/AApoCIII

Although there were five rare subtypes (ACys/Aβ2M/AApoAII/AApoCII/AApoCIII) were not sampled in this study, we analyzed the characteristics of SC distribution of the corresponding amyloid proteins (CYTC/B2MG/APOA2/APOC2/APOC3). These proteins all showed very low abundance across the specimens, especially for CYTC and APOC2 were only identified twice and once respectively (Fig. 1a). Thus it was supposed that these subtypes may also follow the Mayo's rule. However, we can not exclude the possibility that they are similar to the way of ALECT2 in alternative.

Immunoglobulin light chain related amyloidosis (AL/AHL)

In Igκ related amyloidosis (ALκ and AHL (IgGκ)), the SC of Igκ was almost always the highest except in one case that was exceeded by FIBA, and was always higher than Igλ. Whereas in Igλ related amyloidosis (ALλ and AHL (IgGλ/IgAλ)), the SC of Igλ has no such significant superiority as Igκ in Igκ related amyloidosis, it was even sometimes less than Igκ, FIBA or APOA1 (Fig. 1a, 2a). Meanwhile, obivious preponderance of Igκ SC over Igλ in neither Igκ nor Igλ related cases was observed (Fig. 2a). Thus the specimens (ALECT2 cases were excluded) were then divided into three groups: κ-related, including ALκ and Igκ related AHLs; λ-related, including ALλ and Igλ related AHLs; and non-κ/λ related groups, for comparison of Igλ SC minus Igκ SC (λ-κ). As shown in Fig. 2b, there was significant difference of λ-κ between any two of the three groups. In κ-related group, the median value of λ-κ was -10.80 (IQR, -15.60 - -6.81); In non-κ/λ group, it was -3.65 (IQR, -5.24 - -2,12); and in λ-related group, it was 2.02 (IQR, 0.97 - 3.48). There were two cases with the lowest λ-κ value that may interfere the judgement of Igκ

involvement in amyloid deposition, they were AApoAI and AFib respectively. After removing these two cases, the cut-off could be set to -5.45 to achieve the highest sensitivity and specificity in discriminating Igκ involvement. Whereas for judging Igλ involvement, the cut-off could be -0.80.

Immunoglobulin heavy chain related amyloidosis (AH/AHL)

It is a great challenge to discriminate the participation of Immunoglobulin heavy chains in amyloid deposition from AL case, especially for the involvement of IgG for its relatively high abundance in background. To answer this question, we introduced a second superiority score for Immunoglobulin heavy chains (H-score) as illustrated in method. The median value of IgG H-score in non-IgG related amyloidosis was 0.77 (IQR, 0.50 - 0.90), which was significantly higher than IgA H-score in non-IgA related cases (0.20 (IQR, 0.08 - 0.33)) and IgM H-score in non-IgM related cases (0.13 (IQR, 0.03 - 0.24)) (Fig. 3a-c). The cut-off value of IgG H-score to judge IgG involvement could be set to 1.39 to achieve the highest sensitivity and specificity in the training dataset (Fig. 3a), while that of IgA and IgM could be set to 1 for easy to analyze, and also fitted the statistical results (Fig. 3b, c), though we didn't identify IgM related cases to determine the optimal cut-off value with totally confident.

Stepwise data interpretation procedure for amyloidosis subtyping

Based on the characteristics of SC distribution of amyloid proteins in training dataset, we established a data interpretation procedure for amyloidosis subtyping as illustrated in Fig. 4. Firstly, the S-scores of non-immunoglobulin amyloid proteins were analyzed, if any of the S-scores exclusively exceeds its cut-off value, the corresponding subtype would be determined. Scondly, for immunoglobulin amyloidosis, λ-κ value is analyzed to judge the involvement of immunoglobulin light chains. If λ-κ <-5.45, it is assigned to κ-related group; if λ-κ >-0.80, it is assigned to λ-related group. Thirdly, to judge the involvement of immunoglobulin heavy chains, H-scores of IgG/IgA/IgM were analyzed. If any of the H-scores exclusively exceeds its cut-off value, the corresponding involvement of immunoglobulin heavy chain would be determined. If both immunoglobulin light and heavy chains' involvement are recognized, it would be assigned to the corresponding AHLs accordingly.

Performace of the amyloidosis subtyping procedure on validation dataset

The established process was then used to subtyping the 50 collected validation specimens, which achieved a 88% accuracy (Table 3). In detail, 3 ALECT2, 3 AGel, 2 AA, 1 ATTR, 12 ALκ, 15 ALλ, 2 AH (IgG), 4 AHL (IgGλ), 2 AHL (IgAλ) were successfully classified, and an ALκ and an ALλ were failed to be identified, an ALλ and an AHL (IgGλ) were misclassified as AHL (IgGλ) and ALλ respectively, an AHL (IgAλ) and an AH (IgG) were interfered by AHL (IgGλ) and AH (IgG) respectively (Supplementary Table 1-4).

Table 3
LMD-MS subtyping results of validation set by utilizing the data interpretation process.

Subtype							AH	AHL	
	ALECT2	AGel	AA	ATTR	ALκ	ALλ	IgG	IgGλ	IgAλ
Number	3	3	2	1	13	17	3	5	3
Correctly subtyped	3	3	2	1	12	15	2	4	2
Accuracy	100%	100%	100%	100%	92%	88%	67%	80%	67%
Total accurancy	88%								

Diagnostic value for amyloidosis of accompanying proteins

As proposed by Vrana et al., clinical diagnosis of amyloidosis by MS-based proteomics could be achieved by identifying at least two out of the three accompanying proteins (APOE, APOA4 and SAMP) [14]. In our experiment, we also observed that the accompanying proteins were widely present at amyloid deposition sites (Fig. 5a), however, they were also always identified in glomerulus with other renal diseases, which indicate Vrana's method would result in extremely high false positives. Nevertheless, these accompanying proteins had a significant abundance superiority in amyloidosis specimens then in non-amyloid nephropathies. To establish a better diagnostic indicator, receiver operating curves (ROC) for normalized SC of each of the three accompanying proteins and their average value were analyzed using the 94 amyloidosis specimens compared with 55 non-amyloid nephropathies. As expected, the average value showed the highest area under the ROC (AUROC) value of 0.966 (95% confidence interval [CI], 0.941-0.990). Among the single indicators, APOE had the best accuracy, with AUROC of 0.945 (95% CI, 0.905-0.984), followed by 0.934 (95% CI, 0.895-0.973) for SAMP and 0.911 (95% CI, 0.865-0.956) for APOA4 (Fig. 5b).

Discussion

Currently, the LMD-MS based amyloidosis subtyping is increasingly accepted as a clinical test. However, how to read the MS data properly and make the appropriate diagnosis is still a challenge for clinicians. In this study, we adopted a stepwise data interpretation procedure that include or exclude the subtypes group by group. In which, non-immunoglobulin amyloidosis are firstly included or excluded by analyzing the P-scores, followed by considering whether and which immunoglobulin light chain is involved by λ-κ, and lastly, whether and which immunoglobulin heavy chain participated in amyloid deposition was judged by analyzing the H-scores. This procedure was verified to have a accuracy rate of 88% in validation phase.

Of the 7 ALECT2 cases in this study, the SC of LECT2 was relatively low (absolute SC ranged from 3-16 and normalized SC ranged from 1.01-4.22), and were always lower than Igκ and IgG. This was similar to the results reported by Li et al. [22] and Mereuta et al. [29]. These results implied that the abundance of

LECT2 may be underestimated by shot gun proteomics quantification. In addition, LECT2 was not identified in all other non-ALECT2 cases and non-amyloid nephropathies. Therefore, the subtyping of ALECT2 can be determined by the identification of LECT2 confidently.

The major amyloidosis subtype is AL, which is further subdivided into ALκ and ALλ. Thus, the accurate subtyping of AL is an important part of subtyping of amyloidosis. The background of Igκ was relatively high, especially in some AL (Igλ) cases, it was even slightly higher than Igλ. Here, we innovatively proposed the variable of λ-κ to distinguish the interference between Igκ and Igλ, and found that non-κ/λ related categories can be effectively identified by this variable (except for AFib and AApoAI, which could be recognized before λ-κ analysis). In validation dataset, there was only one AL (Igκ) case that had the λ-κ value (-4.06) a little higher than cutt-off (-5.45) and was not recognized immediately. Yet, none of the other subtype was assigned to this case. Other than that, the λ-κ analysis is perfect for distinguishing κ, λ and non-κ/λ related cases.

Amyloid deposition of immunoglobulin heavy chain is usually accompanied with light chain named AHL. This brings a big challenge to distinguish AH and AHL from each other. What's more, in some AL cases, the SC of IgG may have a higher value over light chains, which causes the confusion of AH, AHL and AL. Therefore, we introduced another score (H-score) to recognize the involvement of immunoglobulin heavy chain, especially for IgG. Of the total 51 AL specimens, 5 (9.8%) had higher IgG SC than light chains, which may be easily misclassified to IgG related subtypes. This phenomenon was not observed for IgA and IgM. This may be due to the high background of IgG in the blood that causes interference, and thus the analysis for IgG should be different from IgA & IgM. Consequently, We found that the H-score cut-off for IgG was higher than IgA & IgM. Despite the utilization of H-score, several mistakes were generated (Fig. 3 and Table 3). Among which, the SC of IgG was overrepresented in an AL (Igλ) case and was underrepresented in an AHL (IgGλ) case, as well as in an AHL (IgAλ) case, IgG and IgA both exceeded their cut-off, and in an AH (IgG) case, contradiction happened between IgG and IgM. These mistakes were all associated with IgG, requiring the subtyping method to be further improved in this respect. Also, these cut-off values may need to be optimized by more clinical specimens in future study. For now, it might be better to take a look at histopathological or hematological test results and rely on experienced clinicopathologists to determine whether and which heavy chain is involved. Nevertheless, these mistakes have little influence on the formulation of clinical treatment plan.

Qualitative analysis of accompanying proteins is not an appropriate method to diagnose amyloidosis, since it could not excluded other renal diseases. This may be mainly because of the development of MS technology, which becomes more sensitive and can identify more proteins in lower abundance. Here, we proposed the quantitative analysis way that use the average abundance of the three accompanying proteins, and indicated it as a fine indicator to diagnose amyloidosis.

There were still several rare subtypes such as ACys, Aβ2M, AApoAII, AApoCII and AApoCIII that were not included in this study. This was mainly because of the low incidence of systemic amyloidosis (10 per million) and even lower for rare subtypes. The data interpretation process will be further verified and

optimized in future clinical tests and follow-up studies, as well as the MS data characteristics of these not included subtypes are to be determined more detailly in the future.

Conclusions

This study demonstrates the value of LMD-MS technique for precise diagnosis of amyloidosis. The method of data interpretation is discussed systematically, the principle and stepwise process of MS data analysis that can improve subtyping accuracy was proposed for the first time, where some cut-off values are defined and set. This subtyping scheme includes not only the diagnosis of AL amyloidosis, but also the rare subtypes, which has a high clinical practical value. The development of this method will be helpful for clinicians to accurately diagnose amyloidosis.

Abbreviations

AA: Serum amyloid A amyloidosis; AApoAII: amyloidosis; AApoCII: amyloidosis; AApoCIII: amyloidosis; Aβ2M: amyloidosis; ACys: Cystatin-C amyloidosis; AFib: Fibrinogen α chain amyloidosis; AGel: Gelsolin amyloidosis; AH: Immunoglobulin heavy chain amyloidosis; AHL: Immunoglobulin heavy-light chain amyloidosis; AL: Immunoglobulin light chain amyloidosis; ALECT2: Leukocyte chemotactic factor-2 amyloidosis; ALκ: AL, κ-type; ALλ: AL, λ-type; APOA1: Apolipoprotein A-I; APOA2: Apolipoprotein A-II; APOA4: Apolipoprotein A-IV; APOC2: Apolipoprotein C-II; APOC3: Apolipoprotein C-III; APOE: Apolipoprotein E; ATTR: Transthyretin amyloidosis; AUROC: Area under receiver operating curve; CR: Congo red; B2MG: Beta-2-microglobulin; CYTC: Cystatin-C; DN: Diabetic nephropathy; FFPE: Formalin fixed paraffin-embedded; FGN: Focal glomerulonephritis; FIBA: Fibrinogen α chain; FIBB: Fibrinogen β chain; FIBG: Fibrinogen γ chain; H-score: Superiority of immunoglobulin heavy chain over light chain; IgAN: IgA nephropathy; IQR: Interquartile range; LMD-MS: Laser microdissection combined with mass spectrometry; LN: Lupus nephritis; LYSC: Lysozyme C; MN: Membranous nephropathy; pC: Para-carcinoma; SAA1: Serum amyloid A-1; SAMP: Serum amyloid P component; SC: Spectral count; S-score: Superiority score of non-immunoglobulin amyloid proteins; TTHY: Transthyretin.

Declarations

Ethics approval and consent to participate

All methods in this research were carried out in accordance with the relevant national regulations, institutional policies, and in accordance with the tenets of the Helsinki Declaration. All clinical and laboratory patient data were abstracted in de-identified form, the waiver for informed consent for this study has been approved by the Ethics Committee of *Guangzhou KingMed Diagnostics* and meets the ethical requirements, the approval number is: 2020-041.

Consent for publication

Not applicable.

Availability of data and materials

Data supporting the results are reported in this article and additional information is available. In addition, relevant materials used in the study are available from the corresponding author on reasonable request.

Competing interests

Authors state no conflict of interest.

Funding

No funding exists regarding this manuscript.

Authors' contributions

All authors gave substantial contributions to conception and design, drafting and critical revision of the manuscript. Beibei Zhao, Xin Li and Ming Ke proposed the idea and study design; Xin Li performed the LMD-MS experiments; Lin Wang and Shuling Yue reviewed the specimens, confirmed their subtypes and helped organize thoughts of the manuscript; Ming Ke analyzed and interpreted the data, and was the major contributor in writing the manuscript. Beibei Zhao revised the manuscript to the final edition. All authors read and approved the final manuscript.

Acknowledgements

We would like to acknowledge pathologist Anlan Chen for her participation in confirming the subtype of all the clinial specimens.

References

1. Wechalekar AD, Gillmore JD, Hawkins PN. Systemic amyloidosis. Lancet. 2016, 387(10038): 2641–2654.
2. Hazenberg BP. *Amyloidosis: a clinical overview*. *Rheumatic Disease Clinics of North America*. 2013, *39*(*2*): *323-45*.
3. Benson MD, Buxbaum JN, Eisenberg DS, Merlini G, Saraiva MJM, Sekijima Y, Sipe JD, Westermark P. Amyloid nomenclature 2020: update and recommendations by the International Society of Amyloidosis (ISA) nomenclature committee. Amyloid. 2020, 27(4): 217–222.
4. Merlini G, Dispenzieri A, Sanchorawala V, Schönland SO, Palladini G, Hawkins PN, Gertz MA. Systemic immunoglobulin light chain amyloidosis. Nature Reviews Disease Primers. 2018, 4(1): 38.
5. Murphy C, Wang S, Kestler D, Larsen C, Benson D, Weiss D, Solomon A. Leukocyte chemotactic factor 2 (LECT2)-associated renal amyloidosis. Amyloid. 2011, 18(Suppl 1): 223–225.
6. Picken MM. The Pathology of Amyloidosis in Classification: A Review. Acta Haematol. 2020, 143(4): 322–334.

7. Ebert EC, Nagar M. Gastrointestinal manifestations of amyloidosis. American Journal of Gastroenterology. 2008, 103(3):776–787.
8. Westermark GT, Fändrich M, Westermark P. AA amyloidosis: pathogenesis and targeted therapy. Annual Review of Phytopathology. 2015, 10: 321–344.
9. Martinez-Naharro A, Hawkins PN, Fontana M. Cardiac amyloidosis. Clinical Medicine. 2018(Suppl 2): s30-s35.
10. Gupta N, Kaur H, Wajid S. Renal amyloidosis: an update on diagnosis and pathogenesis. Protoplasma. 2020, 257(5): 1259–1276.
11. Papa R, Lachmann HJ. Secondary, AA, Amyloidosis. Rheumatic Disease Clinics of North America. 2018, 44(4): 585–603.
12. Khoor A, Colby TV. Amyloidosis of the Lung. Archives of Pathology & Laboratory Medicine. 2017, 141(2): 247–254.
13. Howie AJ, Brewer DB, Howell D, Jones AP. Physical basis of colors seen in Congo red-stained amyloid in polarized light. Laboratory Investigation. 2008, 88(3): 232–242.
14. Picken MM. Proteomics and mass spectrometry in the diagnosis of renal amyloidosis. Clinical Kidney Journal. 2015, 8(6): 665–672.
15. Rodriguez FJ, Gamez JD, Vrana JA, Theis JD, Giannini C, Scheithauer BW, Parisi JE, Lucchinetti CF, Pendlebury WW, Bergen HR 3rd, Dogan A. Immunoglobulin derived depositions in the nervous system: novel mass spectrometry application for protein characterization in formalin-fixed tissues. Laboratory Investigation. 2008, 88(10): 1024–1037.
16. Lavatelli F, Valentini V, Palladini G, Verga L, Russo P, Foli A, Obici L, Sarais G, Perfetti V, Casarini S, Merlini G. Mass spectrometry-based proteomics as a diagnostic tool when immunoelectron microscopy fails in typing amyloid deposits. Amyloid. 2011, 18(Suppl 1): 64–66.
17. Brambilla F, Lavatelli F, Di Silvestre D, Valentini V, Rossi R, Palladini G, Obici L, Verga L, Mauri P, Merlini G. Reliable typing of systemic amyloidoses through proteomic analysis of subcutaneous adipose tissue. Blood. 2012, 119(8): 1844–1847.
18. Vrana JA, Gamez JD, Madden BJ, Theis JD, Bergen HR 3rd, Dogan A. Classification of amyloidosis by laser microdissection and mass spectrometry-based proteomic analysis in clinical biopsy specimens. Blood. 2009, 114(24): 4957–4959.
19. Theis JD, Dasari S, Vrana JA, Kurtin PJ, Dogan A. Shotgun-proteomics-based clinical testing for diagnosis and classification of amyloidosis. Journal of Mass Spectrometry. 2013, 48(10): 1067–1077.
20. Dogan A. Amyloidosis: Insights from Proteomics. Annual Review of Phytopathology. 2017, 12: 277–304.
21. Sun W, Sun J, Zou L, Shen K, Zhong D, Zhou D, Sun W, Li J. The Successful Diagnosis and Typing of Systemic Amyloidosis Using A Microwave-Assisted Filter-Aided Fast Sample Preparation Method and LC/MS/MS Analysis. PLoS One. 2015, 10(5): e0127180.

22. Li DY, Liu D, Wang SX, Yu XJ, Cui Z, Zhou FD, Zhao MH. Renal leukocyte chemotactic factor 2 (ALECT2)-associated amyloidosis in Chinese patients. Amyloid. 2020, 27(2): 134–141.
23. Said SM, Sethi S, Valeri AM, Leung N, Cornell LD, Fidler ME, Herrera Hernandez L, Vrana JA, Theis JD, Quint PS, Dogan A, Nasr SH. Renal amyloidosis: origin and clinicopathologic correlations of 474 recent cases. Clinical Journal of the American Society of Nephrology. 2013, 8(9): 1515–1523.
24. Abe R, Katoh N, Takahashi Y, Takasone K, Yoshinaga T, Yazaki M, Kametani F, Sekijima Y. Distribution of amyloidosis subtypes based on tissue biopsy site - Consecutive analysis of 729 patients at a single amyloidosis center in Japan. Pathology International. 2021, 71(1): 70–79.
25. Taylor GW, Gilbertson JA, Sayed R, Blanco A, Rendell NB, Rowczenio D, Rezk T, Mangione PP, Canetti D, Bass P, Hawkins PN, Gillmore JD. Proteomic Analysis for the Diagnosis of Fibrinogen Aα-chain Amyloidosis. Kidney International Reports. 2019, 4(7): 977–986.
26. Nasr SH, Said SM, Valeri AM, Sethi S, Fidler ME, Cornell LD, Gertz MA, Dispenzieri A, Buadi FK, Vrana JA, Theis JD, Dogan A, Leung N. The diagnosis and characteristics of renal heavy-chain and heavy/light-chain amyloidosis and their comparison with renal light-chain amyloidosis. Kidney International. 2013, 83(3): 463–470.
27. Vrana JA, Theis JD, Dasari S, Mereuta OM, Dispenzieri A, Zeldenrust SR, Gertz MA, Kurtin PJ, Grogg KL, Dogan A. Clinical diagnosis and typing of systemic amyloidosis in subcutaneous fat aspirates by mass spectrometry-based proteomics. Haematologica. 2014, 99(7): 1239–1247.
28. Alexander MP, Dasari S, Vrana JA, Riopel J, Valeri AM, Markowitz GS, Hever A, Bijol V, Larsen CP, Cornell LD, Fidler ME, Said SM, Sethi S, Herrera Hernandez LP, Grande JP, Erickson SB, Fervenza FC, Leung N, Kurtin PJ, Nasr SH. Congophilic Fibrillary Glomerulonephritis: A Case Series. American Journal of Kidney Diseases. 2018, 72(3):325–336.
29. Mereuta OM, Theis JD, Vrana JA, Law ME, Grogg KL, Dasari S, Chandan VS, Wu TT, Jimenez-Zepeda VH, Fonseca R, Dispenzieri A, Kurtin PJ, Dogan A. Leukocyte cell-derived chemotaxin 2 (LECT2)-associated amyloidosis is a frequent cause of hepatic amyloidosis in the United States. Blood. 2014, 123(10): 1479–1482.

Figures

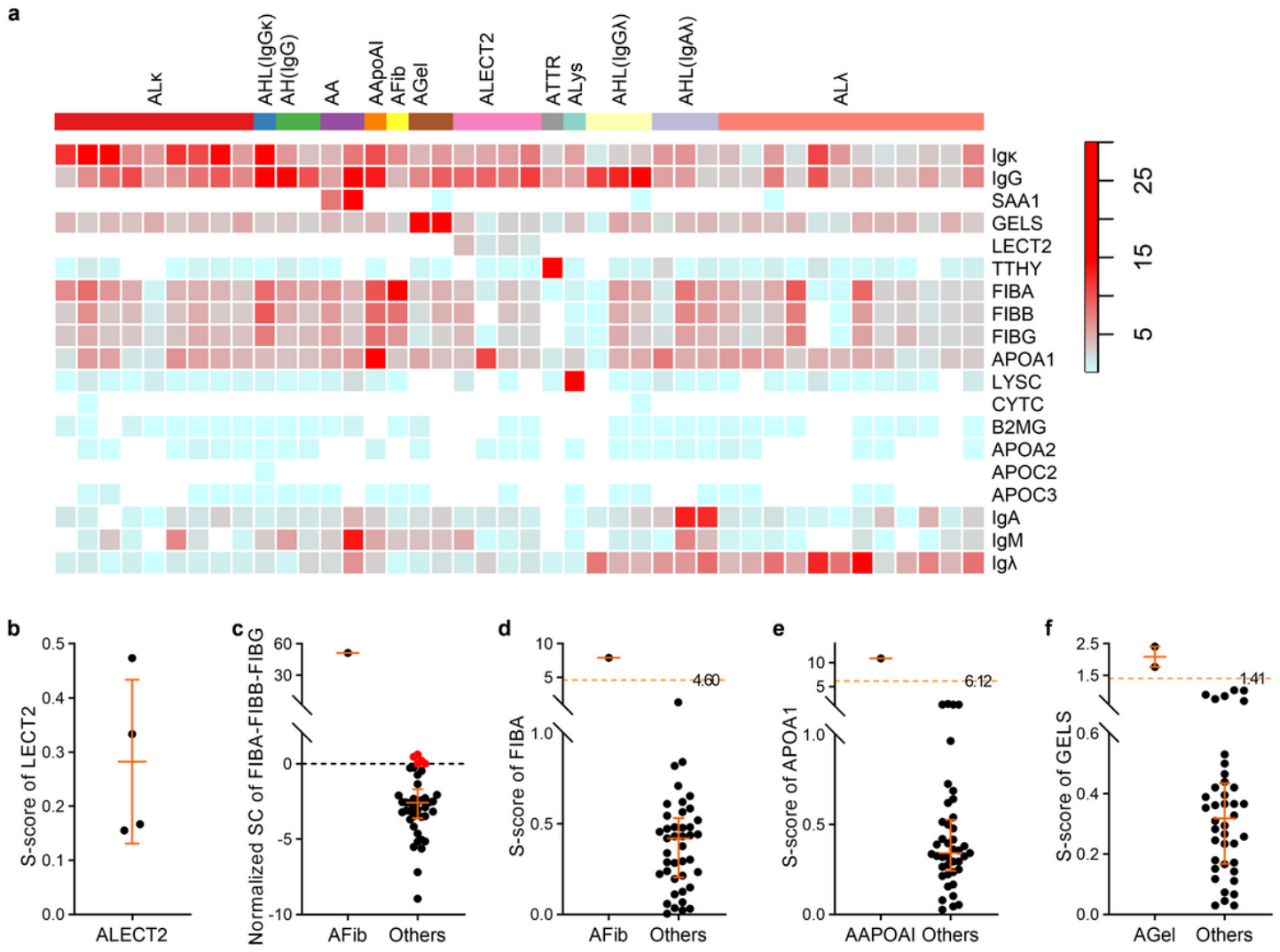

Figure 1

Amyloid protein profile and quantitative analysis of irregular ones. a. Normalized SCs of all the amyloid proteins in each training specimen are presented as heatmap. Subtypes of the cases are labeled by column, and proteins are labeled by row. b. Distribution of LECT2 S-score in ALECT2 cases. c. Scatter plot of normalized SC of FIBA minus the sum of FIBB and FIBG in AFib and non-AFib subtypes. d-f. Comparison of S-scores of FIBA (d), APOA1 (e) and GELS (f) in these amyloid protein involved and irrelevant subtypes. Median with interquartile range of the data is plotted.

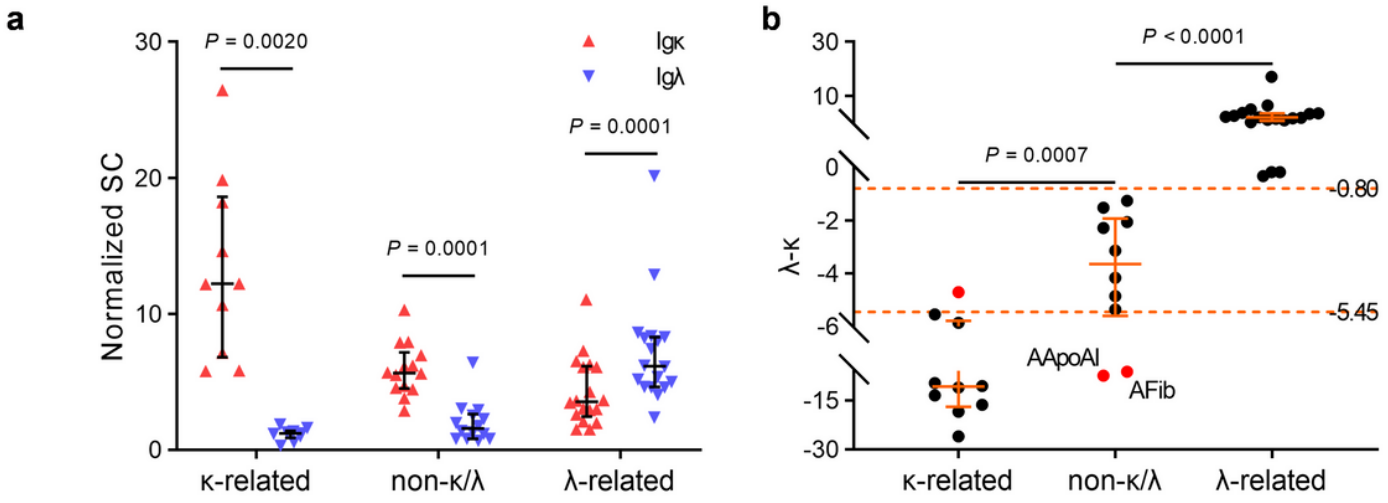

Figure 2

Analysis of the involvement of immunoglobulin light chain in amyloidosis. a. Specimens are divided into three groups: κ-related, λ-related and non-κ/λ, according to whether their amyliod deposition are associated with Igκ, Igλ or neither. In each group, the normalized SC of Igκ and Igλ are compared, with two-sided P values from paired Wilcoxon rank test labeled. b. The λ-κ value that equals Igλ SC minus Igκ SC, is compared among κ-related, λ-related and non-κ/λ groups, with two-sided P values from Mann-Whitney U test labeled. Median with interquartile range of the data is plotted.

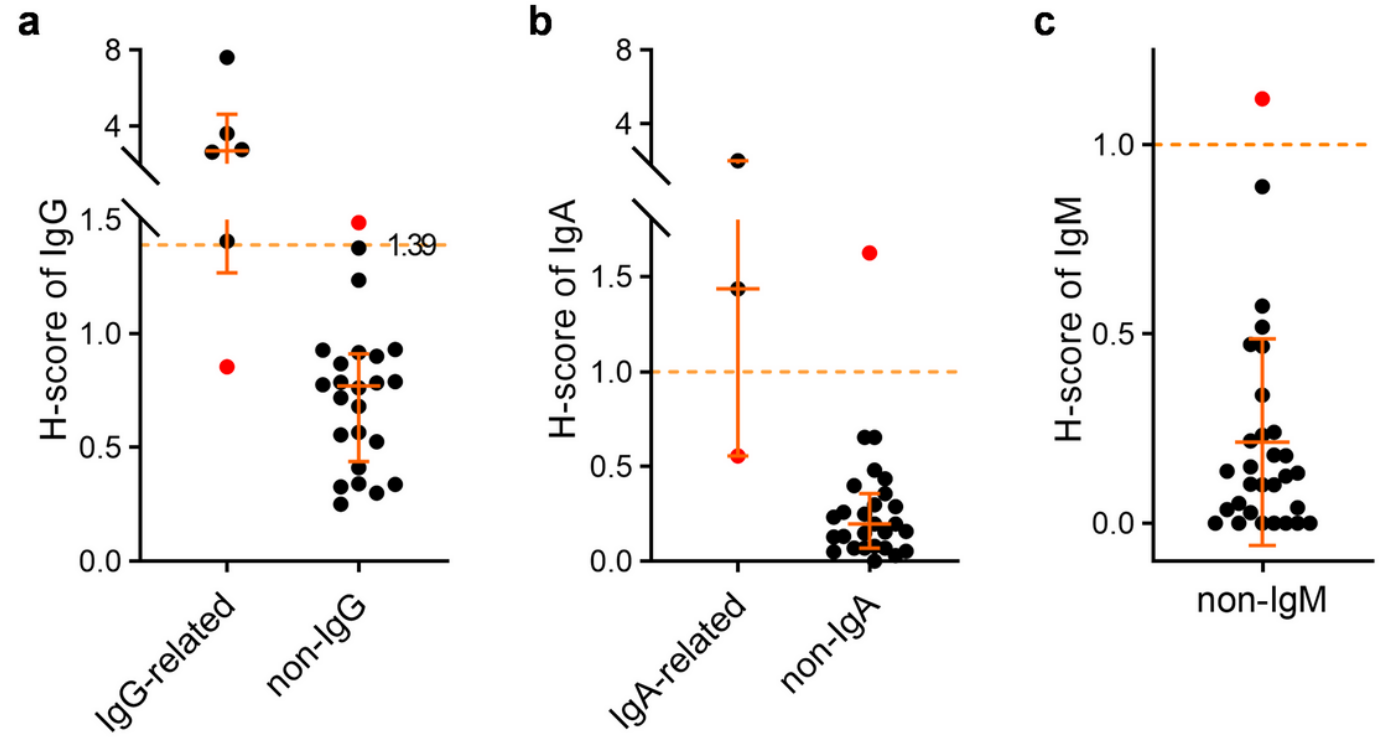

Figure 3

Analysis of the involvement of immunoglobulin heavy chain in amyloidosis. a, b. Comparison of H-scores of IgG (a) and IgA (b) in the immunoglobulin heavy chain involved and irrelevant subtypes. c. Distribution of IgM H-score in non-IgM involved cases. Median with interquartile range of the data is plotted.

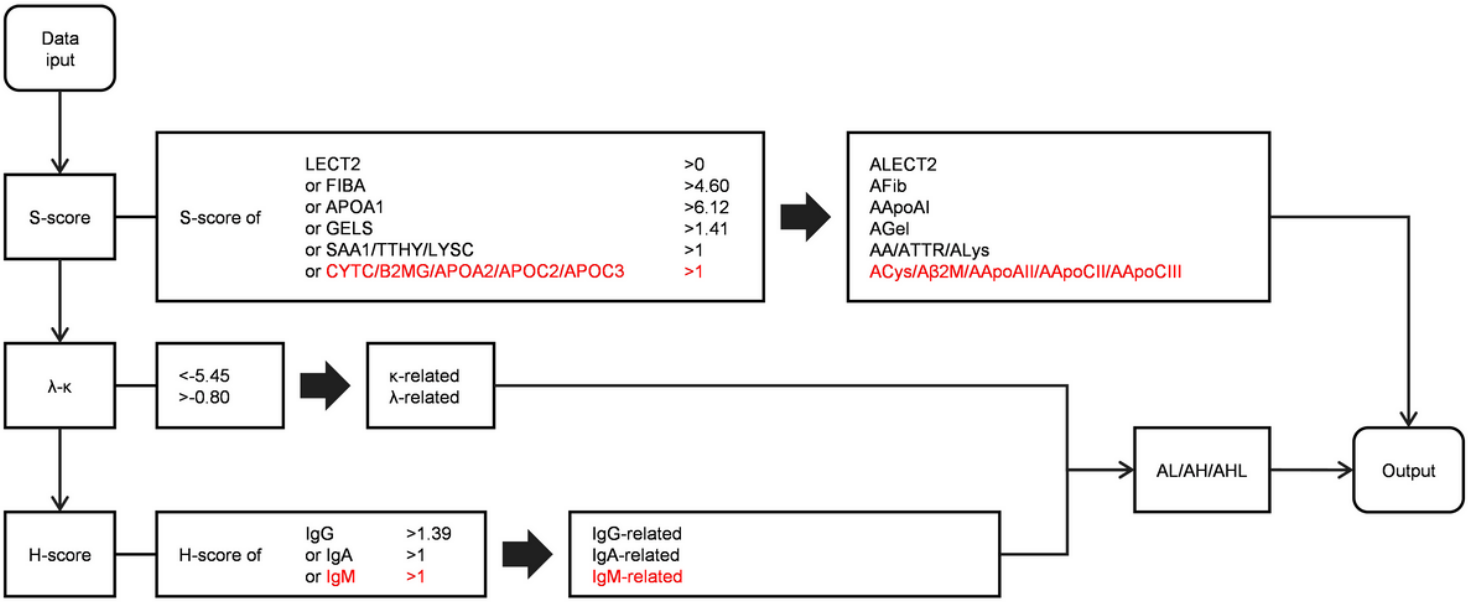

Figure 4

The stepwise data interpretation procedure for amyloidosis subtyping.

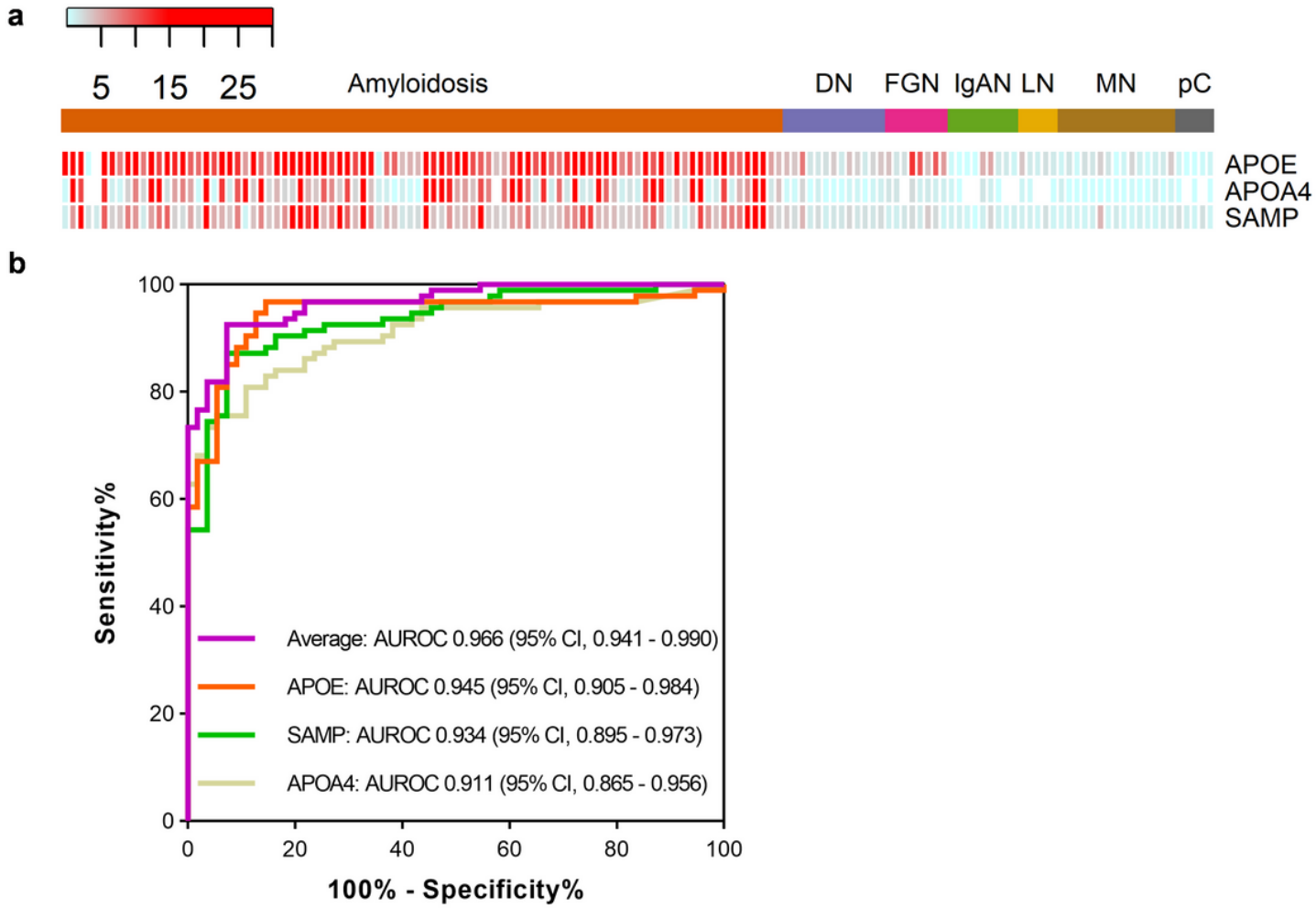

Figure 5

Diagnosis of amyloidosis by quantitative analysis of accompanying proteins. a. Normalized SCs of the three amyloid accomanying proteins in each amyloidosis and non-amyloid nephropathy sample are presented as heatmap. Subtypes of the cases are labeled by column, and proteins are labeled by row. b. Area under the receiver operating curve (AUROC) with respect to normalized SC of accompanying proteins in amyloidosis versus non-amyloid nephropathy. All the three accompanying proteins and their average SC value are used to generate the AUROC curve.

Supplementary Files

This is a list of supplementary files associated with this preprint. Click to download.

- SupplementaryFigure1.tif
- SupplementaryFigure2.tif
- SupplementaryLegends.docx
- SupplementaryTable1.NormalizedSCofamyloidproteinsofvalidationspecimens.xlsx

- SupplementaryTable2.Sscorecalculationinvalidationset.xlsx
- SupplementaryTable3.calculationofimmunoglobulinrelatedamyloidosisinvalidationset.xlsx
- SupplementaryTable4.Hscorecalculationofimmunoglobulinrelatedamyloidosisinvalidationset.xlsx